Charge Exchange (CEX) Corrections for Electric Propulsion Facilities

IEPC-2025-609

Presented at the 39th International Electric Propulsion Conference, Imperial College London, London,
United Kingdom
14-19 September 2025

Richard A. Obenchain* and Richard E. Wirz[†]

Oregon State University, Corvallis, Oregon, 97331, USA

Tyler Topham; Sophia Bergmann; and John Foster¶

The University of Michigan, Ann Arbor, Michigan 48109, USA

Double-to-single ion ratios taken with $E \times B$ probes require corrections for beam attenuation, primarily due to charge exchange events, to estimate ratios at the thruster exit and to predict in-space operation of the thruster. Here we account for both thruster-borne neutrals and facility neutrals to improve the predictions of the beam at the thruster exit plane and differentiate CEX events in the plume. The relative impact of CEX events between beam ions and neutrals is examined under several thrust and operating conditions. The impacts of neutral ingestion are considered, and steady state flux behavior is discussed.

I. Introduction

The presence of neutral particles in the plume results in charge exchange (CEX) events that can both attenuate the overall plume current and change the doubles-to-singles ratio due to differences in CEX likelihood between single ions and double ions.^{1,2} Several methods for correcting such depletion have been used,^{2,3} with the goal of determining the doubles-to-singles ratio at the thruster exit from current measurements downstream by removing the impact of CEX depletion. In the ideal case, proper corrections performed on measurements taken under the same thruster operating condition but at different facility conditions should predict identical ratios at the thruster exit; the resulting current measurements and ion ratios should approximate spacelike operation for the thruster. Accurate determination of the doubles-to-singles ratio allows for thruster lifetime and erosion estimation for both in-space and in-facility operation.⁴

An experimental campaign conducted in 2023 using the NSTAR thruster examined the doubles-to-singles ratios under several combinations of throttle and pumping conditions.⁵ The initial corrections for charge exchange losses were conducted using the simplified correction method developed by Shastry et al.³ Collision cross-sections were calculated using the fits determined by Miller et al.⁶ The attempt to correct these ratios for CEX events using a simplified correction method failed to return the expected constant thruster behavior for a given throttle level.

The correction calculations developed by Shastry et al. explicitly neglect the charge exchange depletion caused by neutrals exhausted directly by the thruster and neutralizer (the "plume neutrals"). At the given operating conditions for that experiment, the effect of plume neutrals was approximated as on the order of depletion by background neutrals at $10^{-6}Torr$ pressure, while the test cases were executed with background neutral pressures on the order of $10^{-5}Torr$. For the current experiment, the background neutral density corresponded to pressure on the order of 10^{-7} to $10^{-6}Torr$; thus, the correction method must be modified to include the depletion by the plume neutrals.

 $[\]P$ Professor, Nuclear Engineering and Radiological Sciences, jefoster@umich.edu



^{*}PhD. Student, Mechanical, Industrial, and Manufacturing Engineering, obenchar@oregonstate.edu

[†]Exec. Dir. for Aerospace Research Programs, College of Engineering, richard.wirz@oregonstate.edu

[‡]PhD., Nuclear Engineering and Radiological Sciences, tytopham@umich.edu

[§]PhD. Student, Nuclear Engineering and Radiological Sciences, boldlygo@umich.edu

This current effort is a collaboration to re-examine the initial results and improve the corrections by including CEX between ions and plume neutrals to determine the pressure-independent thruster ion current ratio. Additional factors in plume depletion are examined to estimate their impact on the results.

II. Methods

The initial experiment was conducted at the Large Vacuum Test Facility (LVTF) at the University of Michigan in 2023; full experimental details and setup can be found in.⁵ The LVTF is designed for high power electric propulsion testing; thirteen TM1200i pumps and 5 custom-designed cryopanel pumps comprise its extraction capability during test campaigns. The presence of background neutrals within the facility can be controlled by enabling or disabling any of these 18 pumps as needed.

Neutral density and fluxes throughout the facility were determined through free molecular flow simulation using COMSOL Multiphysics. The LVTF facility has been previously modeled as part of a larger vacuum facility study. The simulation uses a two-source approximation, where the ion beam is simulated as emission from hot target surfaces after neutralization while slow neutrals (released through the neutralizer and lost from the thruster itself) are released diffusely from the thruster face. Background neutral density was determined at the same location as in the experiment and constant in the thruster region; additionally, flux to the thruster face was calculated as a reference for neutral ingestion as a confounding factor in comparing beam currents between pressure conditions.

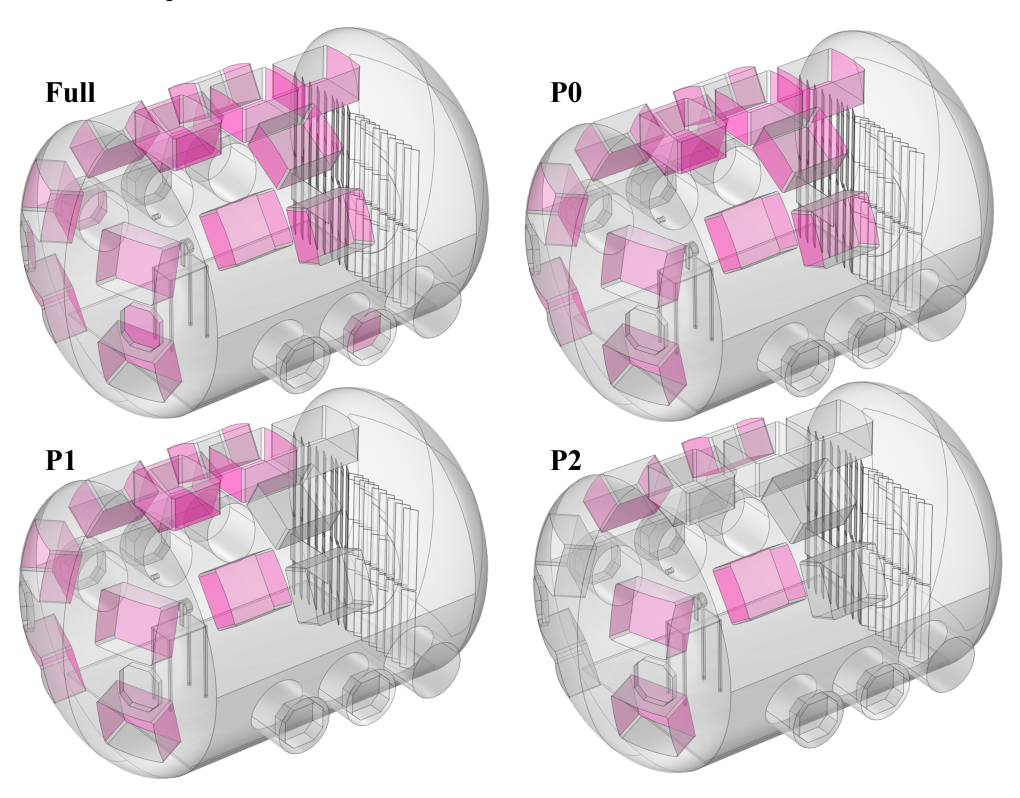


Figure 1: The four pumping configurations of the LVTF used in the experiment and simulation: Full (13 cryopumps and 5 cryopanels operating), P0 (13 cryopumps and 0 cryopanels operating), P1 (10 cryopumps and 0 cryopanels operating).

Four pumping schemes were simulated based on the initial experiment: Full (13 cryopumps and 5 cryopanels operating), P0 (13 cryopumps and 0 cryopanels operating), P1 (10 cryopumps and 0 cryopanels operating), and P2 (5 cryopumps and 0 cryopanels operating). The four pumping configurations are shown in Figure 1, with the active cryopumps and cryopanls highlighted.

Plume neutral density along the z axis was determined numerically through diffusion under cosine distribution across the thruster face in 0.01m steps to the experimental probe distance of 2.08m.

In Figure 2(a), a uniform flux is assumed as emitted from an initial center point on the thruster face at



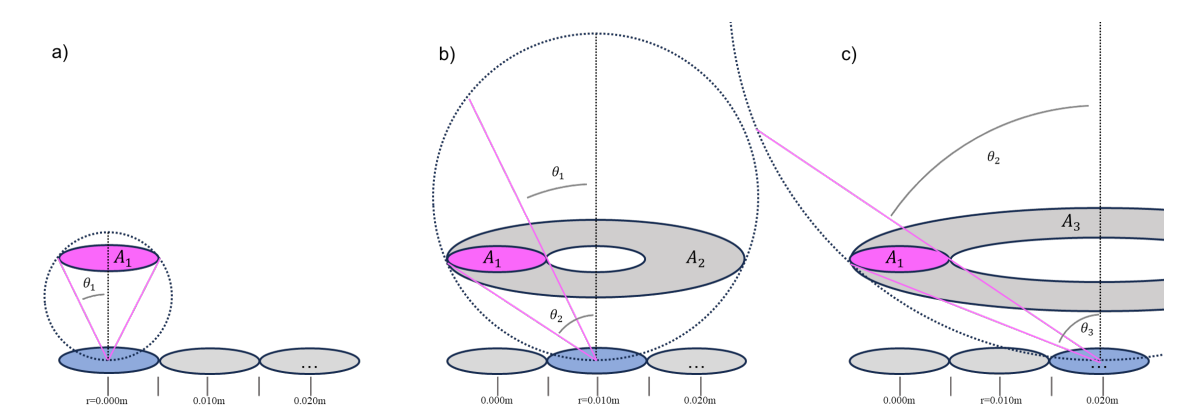


Figure 2: Calculation of the contributions of neutral flux to the center region based on cosine distribution of a uniform flux.

z=0.00m and r=0.00m. At a distance of z=0.01m, the angle from the release point to the outer edge of region with r=0.005m is determined as θ_1 ; the flux of neutrals through this region λ_1 is then calculated relative to the initial uniform flux λ_0 through the release area A_0 as:

$$\lambda_1 = (\lambda_0 * A_1) \sin(\theta_1) / A_1 = \lambda_0 \sin(\theta_1) \tag{1}$$

The next release is considered at point z=0.00m, r=0.01m (Figure 2(b)). The flux λ_2 through the centerline surface A_1 from release point 2 is calculated as a percentage of a projection of flux released from point 2 through annulus A_2 , which is tangential to the near and far edges of A_1 :

$$\lambda_2 = (\lambda_0 * A_2) \frac{A_1}{A_2} [\sin(\theta_2) - \sin(\theta_1)] / A_1 = \lambda_0 [\sin(\theta_2) - \sin(\theta_1)]$$
 (2)

The flux λ_3 from z=0.00m, r=0.02m to surface A_1 is calculated similarly (see Figure 2(c)):

$$\lambda_3 = \lambda_0 [\sin(\theta_3) - \sin(\theta_2)] \tag{3}$$

This is repeated to the edge of the thruster face. The resulting flux through surface A_1 is the sum of these fluxes, which reduces to:

$$\lambda(z) = \lambda_0 sin(\theta_{max}(z)) = \frac{\lambda_0 r_{max}}{\sqrt{r_{max}^2 + z^2}}$$
(4)

The process is then repeated for z = 0.02m to z = 2.08m; Figure 3(a) shows the relative flux strength as a function of axial distance. The incremental flux values are then used to determine the approximate density contribution from plume neutrals at each 0.01m interval.

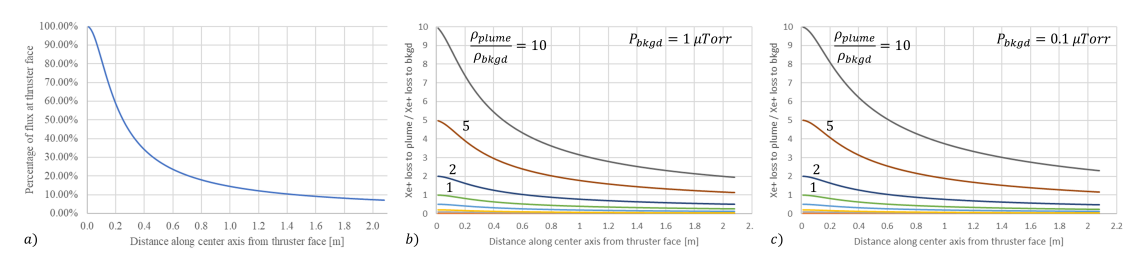


Figure 3: Estimated plume neutral flux along the z-axis as a percentage of plume neutral flux at the thruster face (a). Single ion depletion by plume neutrals normalized to depletion by background neutrals for several plume densities relative to background density for a static background pressure of $1\mu Torr$ (b) and $0.1\mu Torr$ (c).



CEX depletion by plume neutrals was approximated following the method used by Patino and Wirz,² which also uses the cross-sections from Miller et al. The equations for post-depletion currents of singly-and doubly-charged xenon ions j^+ and j^{++} of energy ϵ across some distance from z to z+l due to CEX interactions with neutrals of local density ρ are:

$$j_{z+l}^{+}/j_{z}^{+} = exp(-\sigma_{+}\rho l), \sigma_{+} = [87.3 - 13.6 * log_{10}(\epsilon)] * 10^{-20}$$
(5)

$$j_{z+l}^{++}/j_z^{++} = exp(-\sigma_{++}\rho l), \sigma_{++} = [45.7 - 8.9 * log_{10}(\epsilon)] * 10^{-20}$$
(6)

If the density is constant (such as for background neutrals), then the step size l can be set to the distance z, such that:

$$[j_z^+/j_0^+]_{bkgd} = exp(-\sigma_+\rho_{bkgd}z)$$
 (7)

$$[j_z^{++}/j_0^{++}]_{bkgd} = exp(-\sigma_{++}\rho_{bkgd}z)$$
(8)

If the neutral density ρ is subject to cosine diffusion, the depleted ion currents of energy ϵ at any distance z along the center axis of a thruster with radius r_{max} and initial neutral plume density at the thruster exit ρ_{plume} are then:

$$[j_z^+/j_0^+]_{plume} = \left[\frac{2 * z * (z - \sqrt{z^2 + r_{max}^2})}{r_m a x^2} + 1 \right]^{\gamma^+}, \gamma^+ = 0.5 r_{max} \rho_{plume} \sigma_+$$
 (9)

$$[j_z^{++}/j_0^{++}]_{plume} = \left[\frac{2 * z * (z - \sqrt{z^2 + r_{max}^2})}{r_m a x^2} + 1 \right]^{\gamma^{++}}, \gamma^{++} = 0.5 r_{max} \rho_{plume} \sigma_{++}$$
 (10)

Neutral density for any given position along the z-axis is the sum of the constant background neutral density and the varying plume neutral density, $\rho = \rho_{bkgd} + \rho_{plume}$. The currents resulting from the combined impact of background and plume neutrals are therefore:

$$j_{z+l}^{+}/j_{z}^{+} = [j_{z+l}^{+}/j_{z}^{+}]_{bkgd} * [j_{z+l}^{+}/j_{z}^{+}]_{plume}$$
(11)

$$j_{z+l}^{++}/j_z^{++} = [j_{z+l}^{++}/j_z^{++}]_{bkgd} * [j_{z+l}^{++}/j_z^{++}]_{plume}$$
(12)

Equations 7-12 were solved for each 0.01m step along the z-axis using the density calculated for that distance z. Figure 4 shows the percentage of ions involved in CEX events for the TH10-P2 condition at each position (left axis) and cumulatively (right axis).



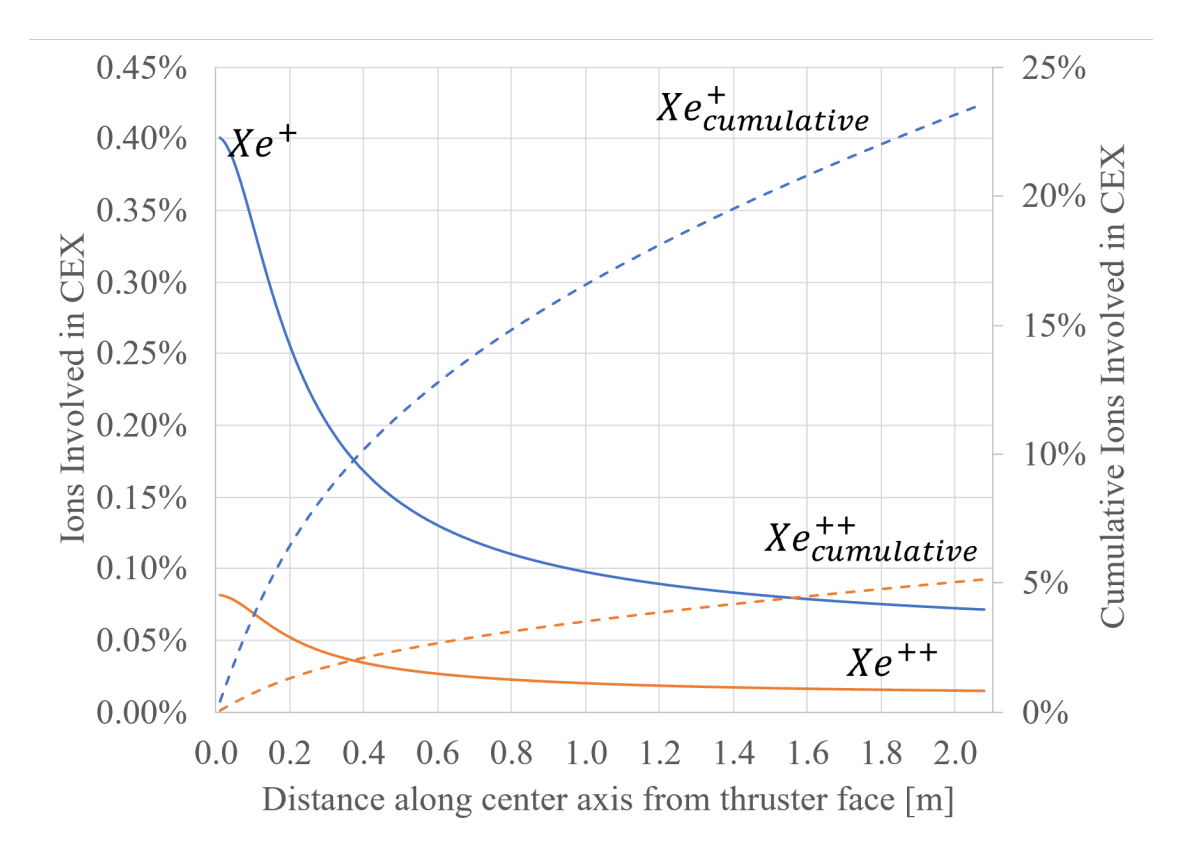


Figure 4: Frequency of CEX events as a percentage of ions for Xe^+ and Xe^{++} and the TH10-P2 operating condition; the instantaneous rate is plotted along the left axis, and the cumulative rate is plotted along the right axis.

III. Results & Analysis

Simulated neutral flux in the vicinity of the thruster was slightly in excess (105% to 110%) of that at the position of the ion gauge; while potentially significant for the purposes of neutral ingestion, the contribution of this additional flux to the overall background neutral density in the most extreme case came to less than 1% variation in the final projected ion currents. Thus, the initial densities determined through the experiment were used for the background neutral density values.

Figure 5 shows the calculated results for two test conditions: (a) and (b) depict predictions under the lowest density condition, with the thruster operating at throttle level TH01 and all pumps and panels active (the Full pump condition); (c) and (d) depict predictions under the highest density condition, with the thruster operating at TH10 and only 5 cryopumps active (the P2 pump condition). For TH01-Full, the experimentally measured background pressure was $0.889\mu Torr$, which was calculated as corresponding to an approximate neutral particle density of $2.86x10^{16}m^{-3}$. Outbound neutral flux near the thruster exit, composed of neutrals lost from the thruster as well as neutral flow from the neutralizer, was approximated through simulation as $1.37x10^{20}s^{-1}m^{-2}$ and corresponded to an approximate exit density of $6.31x10^{17}m^{-3}$; this density was calculated as diffusing to $4.39x10^{16}m^{-3}$ at z=2.08m. Current depletion due to the neutral plume was thus always in excess of that due to background neutrals, which can be seen in Figure 5(b); the cumulative attenuation was calculated to be approximately 15.3%.

For the TH10-P2 condition, the plume neutral density along the z-axis ranged from $7.74x10^{17}m^{-3}$ at the thruster face to $5.38x10^{16}m^{-3}$ at z=2.08m; given the average background neutral density of $1.02x10^{17}m^{-3}$, depletion due to background neutrals begins to dominate at approximately z=0.96m downstream of the thruster face as shown in Figure 5(c). 63% of the total attenuation of 22.7% at z=2.08m (Figure 5(d)) is caused by CEX events with plume neutrals.

As can be seen from these two sample cases, beam depletion due to plume neutrals dominates in all the experimental examples. This is a consequence of relatively low background neutral density: the high pumping



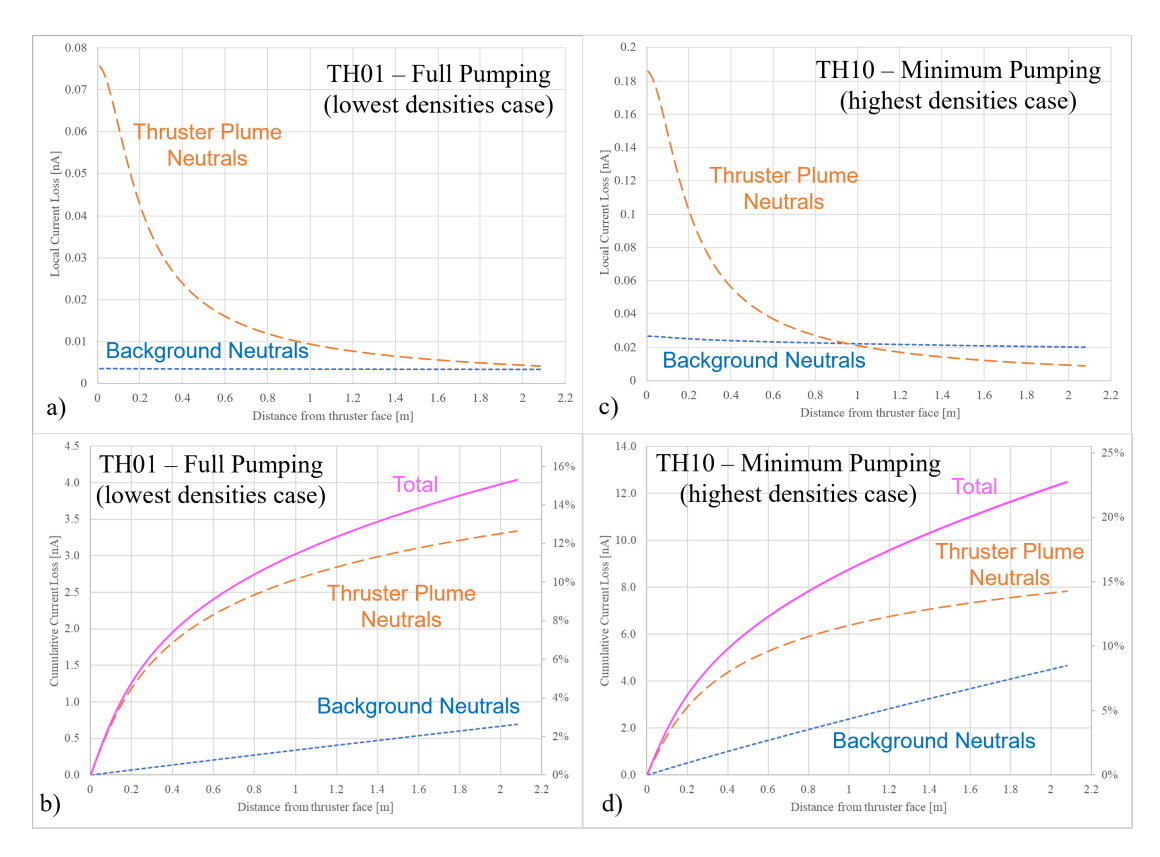


Figure 5: Predictions of current loss and measurement along the z axis. Current losses due to background neutrals and plume neutrals are shown for the minium density case of TH01-Full (a) and the maximum density case of TH10-P2 (c). Similarly, predicted cumulative loss along the z-axis for the background, plume, and cumulative neutral effects are shown for the minium density case of TH01-Full (b) and the maximum density case of TH10-P2 (d). All currents are shown in units of nA; for (b) and (d), the percentage attenuation is shown on the right axis.

capacity of LVTF in combination with the moderate or low mass flow rates for the NSTAR throttle conditions results in lower background neutral presence throughout the facility. There is therefore a lower threshold for plume neutrals to significantly contribute to CEX events in the beam. For example, a neutralizer flow rate of 3sccm translates to a particle flow rate of approximately $1.35x10^{18}s^{-1}$; near the face of the thruster, this alone contributes to a particle density of approximately $1x10^{17}m^{-3}$. While this density will diffuse as z increases, the plume neutrals can no longer be considered insignificant in comparison to background densities that range between $2.9x10^{16}m^{-3}$ and $1x10^{17}m^{-3}$.

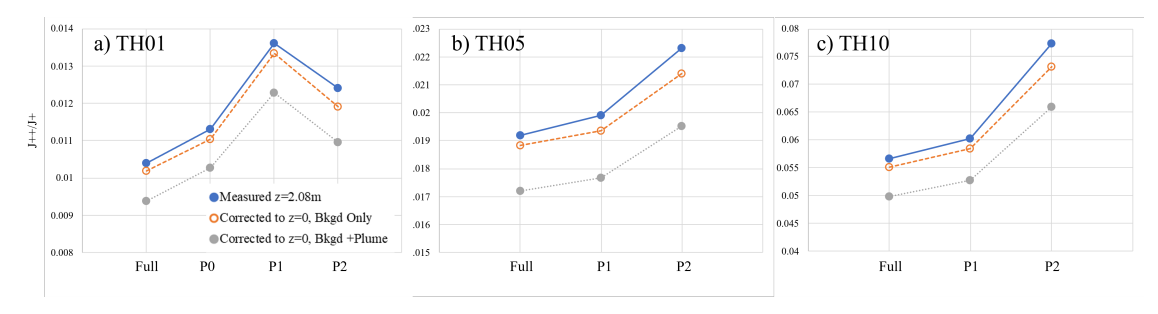


Figure 6: Beam doubles-to-singles ratio (J^{++}/J^+) for the multiple pressure conditions for TH01 (a), TH05 (b), and TH10 (c). For each operating level and pressure condition, three values are shown: the initial measured ratio, the ratio corrected for background neutral CEX events, and ratio corrected for both background and plume neutral CEX events.



The final beam current ratios for each throttle condition are shown in Figure 6. The given ratios include the initial measured ratios at z=2.08m, the initial estimate of the current ratio at z=0m when corrected for CEX events involving only background neutrals, and the estimate of the current ratio at z=0m when corrected for CEX events involving both background and plume neutrals. While correcting for both neutral sources does improve the relative ratios, the trends still differ from the expected constant ratio, especially in the P2 pressure condition. The P0 condition results were removed from the TH05 and TH10 thrust conditions as extreme outliers and therefore suspect data.

As stated in the initial work, some of the remaining discrepancy may be due to ingestion of background neutrals into the thruster; plume neutrals are released from the thruster on forward trajectories and therefore are not expected to contribute to thruster ingestion. The impact of ingested neutrals on thruster operation can generally be quantified by consideration of the ratio of ingested neutrals to thruster exhaust.⁸ For the highest flux case (TH10-P2), flux to the thruster face was simulated as 3% higher than the flux recorded at the ion gauge; this corresponds to a flux of approximately $6.4x10^{18}s^{-1}m^{-2}$. This amounts to 2.1% of the mass flow out of the thruster (which excludes the neutralizer flow) for an approximate ingestion of 0.032%. If 100% of these ingested neutrals are converted to doubles, they would shift the doubles-to-singles ratio for this condition from 0.0660 to 0.0627, which remains significantly higher than the TH10-P1 ratio of 0.05270. Thus, simple mass ingestion is insufficient to account for the remaining current ratio discrepancies.

Further, the projected initial sampled currents from each of the three valid TH10 test conditions of Full, P1, and P2 are 46.38nA, 47.32nA, and 54.95nA respectively. The TH10-P2 case would require an additional 15.6% attenuation to fully counter this difference; such a high attenuation implies a substantial facility effect or interaction.

Analysis of the measured data revealed additional inconsistencies. Simulation of the LVTF facility under each test condition generated simulated static pressure measurements that were approximately half the value measured during the experiment. As an analytical check, we consider the basic steady state mass flow condition. For a given total pump surface area and sticking coefficient, the flux required to maintain steady state will be based on the mass flow into the facility; that is, the average flux to pump surfaces will increase until it is sufficient to balance the mass flow into the facility and thus reach the steady-state condition. For the TH10-P2 case, the total mass flow was 24.16sccm, which is approximately 2.37mg/s. Under the P2 pumping condition, only 5 TM1200i cryopumps were operating; this translates to an exposed pumping surface area of $A_{pump} = 13.5m^2$. For an approximate sticking coefficient of $\alpha_{sc} = 0.26$, this results in a required flux of:

$$\lambda = \frac{\dot{m}_{in}}{A_{pump}\alpha_{sc}} = 6.75x10^{-7}kgs^{-1}m^{-2} = 3.09x10^{18}s^{-1}m^{-2}$$

This background flux is characteristic of the steady-state for this experiment condition and generally represents the minimum flux to be experienced by any open (non-shadowed) surface in the chamber. Upon interaction with an ion gauge, $3.09x10^{18}s^{-1}m^{-2}$ should correspond to roughly $1.76\mu Torr$ of calibrated static pressure, which assumes the flux to density relationship of $\lambda = \frac{n\bar{c}}{4}$. The measured static pressure for the TH10-P2 case was reported as $3.15\mu Torr$, approximately twice the expected value; the simulated pressure at the ion gauge location was given as $1.78\mu Torr$, which is in agreement with the expectation. Similar results are observed for the remaining test conditions; Table 1 shows the background, simulated, and measured values in comparison. The simulated and background values align closely, with the simulated flux values ranging from 95.9% to 115% of the analytically determined background values. The measured values, however, vary from 180% to 404% of the background values. Further, results published by Viges et al. during the characterization of the LVTF's additional pumps indicate consistency with the analytica model and simulated results. 10 While this suggests an additional factor complicating the determination of the flux (and thus densities) within the facility, any correction that reduced the measured flux and pressure values would correspondingly increase the discrepancy in the CEX corrections by reducing attenuation. Additional refinement of both the evolution of the plume and plume characteristics may be possible through more detailed analysis of plume evolution and plume dynamics. 11,12



Table 1: Background, simulated, and experimentally measured flux and pressure values for the test conditions

	Background	Static	Simulated	Static	Measured	Static
Test	flux	Pressure	flux	Pressure	flux	Pressure
condition	$[s^{-1}m^2]$	$[\mu Torr]$	$[s^{-1}m^2]$	$[\mu Torr]$	$[s^{-1}m^2]$	$\mu Torr$
TH01						
Full	4.34E17	0.246	4.58E17	0.246	15.7E17	0.889
P0	5.33E17	0.302	5.58E17	0.318	21.5E17	1.22
P1	7.25E17	0.411	7.43E17	0.420	21.0E17	1.19
P2	14.5E17	0.823	14.2E17	0.789	40.2E17	2.28
TH05						
Full	6.41E17	0.363	7.02E17	0.406	19.7E17	1.12
P0	7.10E17	0.403	7.65E17	0.437	23.6E17	1.34
P1	11.1E17	0.630	11.9E17	0.672	27.5E17	1.56
P2	22.2E17	1.26	22.6E17	1.26	41.4E17	2.35
TH10						
Full	9.18E17	0.521	10.3E17	0.597	25.6E17	1.45
P0	11.8E17	0.669	13.0E17	0.747	29.6E17	1.68
P1	15.5E17	0.878	16.8E17	0.952	32.8E17	1.86
P2	30.9E17	1.76	32.0E17	1.78	55.7E17	3.16

IV. Conclusion

Re-examination of charge exchange corrections applied to experimentally-obtained doubles-to-singles ratios accounted for several gaps in the original effort but failed to fully resolve the apparent discrepancies in predicting in-space operation. The background particle densities in the experiments were on the order of $1 \times 10^{17} m-3$, while the plume neutrals contributed to an equivalent density ranging from $7.74 \times 10^{17} m-3$ to $5.38 \times 10^{16} m-3$ for the highest flow case. CEX depletion due to thruster-borne plume neutrals was thus in excess of that due to background neutrals in all cases. Ratio corrections including the plume neutral depletion came closer to the expected values but were insufficient to completely resolve the predicted thruster behavior. Neutral ingestion into the thruster was determined to be approximately 0.3% of thruster mass flow and closed the gap, but could not account for the remaining discrepancies. Future efforts will include close collaboration between the experiment and model to ensure robust correlation between experimental conditions and model assumptions.

Acknowledgments

The authors acknowledge support from the Joint Advanced Propulsion NASA Space Technology Research Institute. This work was funded by Joint Advanced Propulsion Institute 20-STRI-FULL-0004, NASA Grant Number 80NSSC21K1118.

References

⁵Tyler Topham. Understanding the Mechanisms Affecting Gridded Ion Engine Operation in Ground Test Facilities. PhD thesis, University of Michigan, 2025.



¹J Anderson. Charge-exchange collision effect on e_b probe location for nexis testing. *Internal Memorandum, Jet Propulsion Laboratory, Pasadena, CA*, 2004.

²Marlene I Patino and Richard E Wirz. Characterization of xenon ion and neutral interactions in a well-characterized experiment. *Physics of Plasmas*, 25(6), 2018.

 $^{^3}$ Rohit Shastry, Richard R Hofer, Bryan M Reid, and Alec D Gallimore. Method for analyzing e× b probe spectra from hall thruster plumes. Review of Scientific Instruments, 80(6), 2009.

⁴Christopher M. Cretel and Richard E. Wirz. Electric propulsion mission optimization using reduced order models and data-driven analysis. In 39th International Electric Propulsion Conference, pages IEPC–2025–585, 2025.

- ⁶J Scott Miller, Steve H Pullins, Dale J Levandier, Yu-hui Chiu, and Rainer A Dressler. Xenon charge exchange cross sections for electrostatic thruster models. *Journal of Applied Physics*, 91(3):984–991, 2002.
- ⁷Richard A. Obenchain, Ehsan E. Taghizadeh, and Richard E. Wirz. Collisionless flux-based analyses of neutral drift and transport in hall thruster test facilities. In 39th International Electric Propulsion Conference, pages IEPC–2025–606, 2025.
- ⁸Richard A Obenchain and Richard Wirz. Neutral ingestion compensation for gridded ion thrusters via modeling and analysis. In AIAA SCITECH 2024 Forum, page 1548, 2024.
- ⁹Ehsan E. Taghizadeh, Richard A. Obenchain, Luke K. Franz, and Richard E. Wirz. Electric propulsion facility optimization via reduced order modeling. In 38th International Electric Propulsion Conference, pages IEPC–2024–588, 2024.
- ¹⁰Eric A Viges, Benjamin A Jorns, Alec D Gallimore, and JP Sheehan. University of michigan's upgraded large vacuum test facility. In 36th International Electric Propulsion Conference, pages 1–18, 2019.
- ¹¹Ian Hofbeck and Richard E. Wirz. Spatial spectroscopy for hall thruster plasma species. In 39th International Electric Propulsion Conference, pages IEPC–2025–630, 2025.
- ¹²Andrea Harteloo and Richard E. Wirz. Ultra-fastoes for correlating hall thruster discharge and cathode oscillations. In 39th International Electric Propulsion Conference, pages IEPC-2025-665, 2025.

